

DFT Study of the Olefin Metathesis Catalyzed by Ruthenium Complexes

Fernando Bernardi, Andrea Bottoni,* and Gian Pietro Miscione

Dipartimento di Chimica "G. Ciamician", Università di Bologna, Via Selmi 2,
40126 Bologna, Italy

Received July 8, 2002

A theoretical investigation has been carried out at the DFT (B3LYP) level on the mechanism of the metathesis reaction catalyzed by Grubbs' complexes. Two model systems have been used: (a) The first model is formed by one ethylene molecule and the $\text{Cl}_2(\text{PH}_3)_2\text{-Ru}=\text{CH}_2$ complex (Grubbs' catalyst). (b) In the second model the $\text{Cl}_2(\text{PPh}_3)_2\text{Ru}=\text{CH}_2$ species has been considered. The following results are relevant: (i) The "primary" active catalytic species is a metal-carbene $(\text{PR}_3)_2\text{Cl}_2\text{Ru}=\text{CH}_2$. The corresponding carbenoid complex $(\text{PR}_3)_2\text{-ClRu}-\text{CH}_2\text{Cl}$ is significantly higher in energy (18.45 and 19.26 kcal mol⁻¹ for the two model systems) and thus cannot represent the starting active species of the process. (ii) The existence of three different reaction pathways has been demonstrated. One of the two most likely reaction channels is characterized by the presence of "secondary" active species of carbenoid type. These species, after olefin coordination, become slightly more stable than the corresponding carbenic forms and play a key role in the formation of the metallacyclobutane intermediates. Their stability further increases when phenyl rings replace the phosphine hydrogens. (iv) The cyclopropanation is disfavored since it requires the overcoming of larger activation barriers than those found for the metathesis.

Introduction

Catalyzed olefin metathesis reactions represent one of the most important synthetic processes discovered in the past four decades. This reaction describes the apparent interchange of carbon atoms between two pairs of bonds. The process is schematically represented in Scheme 1, where alkylidene units CHR are exchanged between double bonds. The final result is that each half of the first olefin molecule becomes bonded to either half of the second olefin.^{1–3}

The use of this reaction has become more and more important in recent years and has found considerable applications either in the industry or in the academic laboratories. An example of practical use is the Shell higher olefin process (SHOP) for the large-scale production of long-chain α -olefins.¹ Furthermore, several recent syntheses of a variety of natural and non-natural products are based on ring-closing metathesis to obtain macrocycles otherwise difficult to prepare.⁴

The catalytic systems used for olefin metathesis involve almost invariably transition metal compounds. "First-generation" catalytic systems often require the presence of a cocatalyst, and sometimes a third compound (promoter) must be added to the reaction mixture. The most common systems are based on Mo, Ru,

Scheme 1



W, Re, Os, and Ir. EtAlCl_2 , R_3Al , and R_4Sn are typical cocatalysts, while compounds containing oxygen (O_2 , EtOH , PhOH) can be used as promoters. There is evidence that these catalytic systems lead to the initial formation of metal carbene complexes of the type $[\text{L}]\text{M}=\text{CHR}$ (L = ligand), which would represent the real active catalytic form.

Over the past 15 years, new catalysts based on late transition metals have been proposed. These catalysts are well-defined metal carbene complexes, which can initiate directly all types of olefin metathesis without requiring the presence of a cocatalyst. A substantial contribution to the development of these new catalysts is due to Grubbs and co-workers.^{4a,b,5} These authors used ruthenium carbene complexes $\text{Cl}_2(\text{PR}_3)_2\text{Ru}=\text{CHR}'$ to carry out the metathesis of a number of different olefins such as strained and low-strain cyclic olefins, exocyclic olefins, and straight-chain alkenes. Grubbs' group has carried out detailed studies to elucidate the mechanism of olefin metathesis. In particular a systematic investigation of the $\text{Cl}_2(\text{PCy}_3)_2\text{Ru}=\text{CHPh}$ catalyst has suggested that the most active species should be a 14-electron monophosphinic complex (present for less than 5%) with the biphosphinic complex much less reactive.^{5f,g} The general mechanistic pattern, which stems from these results, is schematically reported in Scheme 2. Here the metathesis reaction proceeds through a series of subsequent equilibria. In a first step the monophosphinic complex coordinates the olefin

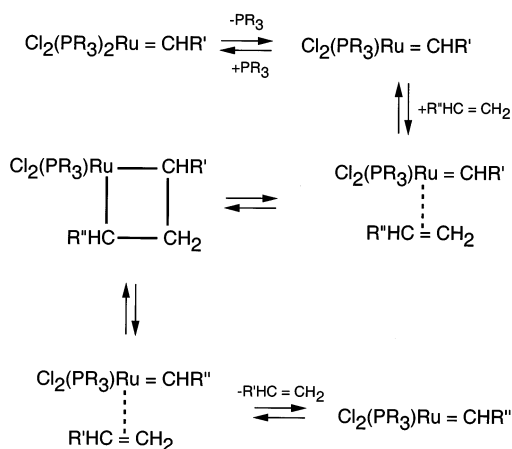
(1) Ivin, K. J.; Mol, J. C. *Olefin Metathesis and Metathesis Polymerization*; Academic Press: New York, 1997.

(2) Katz, T. J. *Adv. Organomet. Chem.* **1978**, *16*, 283.

(3) Calderon, N.; Lawrence, J. P.; Ofstead, E. A. *Adv. Organomet. Chem.* **1979**, *17*, 449.

(4) (a) Miller, S. J.; Kim, S.; Chen, Z.; Grubbs, R. H. *J. Am. Chem. Soc.* **1995**, *117*, 2108. (b) Miller, S. J.; Blackwell, H. E.; Grubbs, R. H. *J. Am. Chem. Soc.* **1996**, *118*, 9606. (c) Xu, Z.; Johannes, C. W.; Hourii, A. F.; La, D. S.; Cogan, D. A.; Hofilena, G. E.; Hoveyda, A. H. *J. Am. Chem. Soc.* **1997**, *119*, 10302.

Scheme 2



(π -bonded complex). This step is followed by the reversible formation of a ruthenacyclobutane. The breaking of the cycle can provide either the original olefin or the final product.

A few years ago a molecular dynamic investigation has been carried out on the metathesis reaction using a model system formed by an ethylene molecule and the $\text{Cl}_2(\text{PH}_3)_2\text{Ru}=\text{CH}_2$ complex.⁶ The results obtained in the molecular dynamic simulations support the mechanism proposed by Grubbs et al.^{5f,g} In particular it has been found that the complex $\text{Cl}_2(\text{PH}_3)_2\text{Ru}=\text{CH}_2$ can lose one phosphine ligand, leading to a small fraction of the monophosphinic species. Also, the formation of a metallacyclobutane intermediate has been observed.

A different mechanistic hypothesis has been proposed by Hofmann and co-workers,⁷ who demonstrated that the reaction proceeds using carbenic ruthenium complexes with chelating bis(di-*tert*-butylphosphanyl)methane. Since in these species the loss of a phosphine ligand is quite difficult, these results suggest that even bis-phosphinic complexes can catalyze the reaction. In this case the coordination of the olefin by the bis-phosphine complex would lead to the formation of an octahedral 18-electron intermediate. Other experimental evidence obtained by these authors indicated carbenoid complexes as possible catalytic species.

More recently a combined theoretical and experimental study on the metathesis promoted by the $\text{Cl}_2(\text{PCy}_2\text{R})_2\text{Ru}=\text{CHPh}$ species has been carried out by Chen and co-workers.⁸ While the quantumchemical computations at different levels of theory (DFT and coupled-clusters) are in agreement with the Grubbs' mechanism, the experimental observations obtained in the gas phase by electrospray ionization tandem mass spectroscopy are

consistent with a reaction profile where the metallacyclobutane is a transition state rather than an intermediate.

In a very recent work the effect of ligand variation on the activity of ruthenium-based catalysts of the general formula $\text{L}(\text{PR}_3)(\text{X})\text{Ru}=\text{CHR}$ has been investigated by Grubbs and co-workers.⁸ The authors concluded that, for the catalysts they have considered, there is no evidence that a reaction pathway involving an 18-electron adduct contributes significantly to the metathesis reaction. This would point to the 14-electron monophosphine complex as the main active species of the reaction.

An interesting paper by Cavallo¹⁰ has just appeared in the literature. The author has carried out a DFT theoretical study of the metathesis reaction using as model systems various types of catalysts (Grubbs' complexes and Hofmann's cationic species) with bulky ligands to include steric effects, which are present in the real system. However, he considered only the reaction path where the coordination of the olefin requires, first, the dissociation of one phosphine (formation of the 14-electron intermediate suggested by Grubbs). No other mechanistic possibilities have been investigated in this study.

Despite the wide application of olefin metathesis and the large number of papers that have appeared in the literature, several mechanistic aspects have not been completely elucidated yet. What is, for instance, the rate-determining step of the process? And the nature of the metallacyclobutane? Is this species a real intermediate or a transition state? Also, what is the structure of the real active catalytic species? How important in these processes is the competition between metathesis and cyclopropanation?

In the present paper, to answer these and other questions and to obtain a detailed mechanistic picture, the metathesis reaction has been carefully investigated at the DFT level. To this purpose a model system formed by the $\text{Cl}_2(\text{PH}_3)_2\text{Ru}=\text{CH}_2$ complex and one ethylene molecule has been considered. Furthermore, since in the real experiments much more cumbersome ligands, such as PCy_3 , PPh_3 , and PPR_3 , are bonded to the metal, to check the reliability of our model system, for several points of the reaction surface both PH_3 ligands have been replaced by triphenylphosphine (PPh_3) groups.

Computational Procedure

All the DFT computations reported here have been performed with the Gaussian 98¹¹ series of programs using the

(5) (a) Nguyen, S. T.; Johnson, L. K.; Grubbs, R. H. *J. Am. Chem. Soc.* **1992**, *114*, 3974. (b) Nguyen, S. T.; Grubbs, R. H. *J. Am. Chem. Soc.* **1993**, *115*, 9858. (c) Schwab, P.; France, M. B.; Ziller, J. W.; Grubbs, R. H. *Angew. Chem., Int. Ed. Engl.* **1995**, *34*, 2039. (d) Schwab, P.; Grubbs, R. H.; Ziller, J. W. *J. Am. Chem. Soc.* **1996**, *118*, 100. (e) Wilhelm, T. E.; Belderrain, T. R.; Brown, S. N.; Grubbs, R. H. *Organometallics* **1997**, *16*, 3867. (f) Dias, E. L.; Nguyen, S. T.; Grubbs, R. H. *J. Am. Chem. Soc.* **1997**, *119*, 3887. (g) Ulman, M.; Grubbs, R. H. *Organometallics* **1998**, *17*, 2484.

(6) Aagaard, O. M.; Meier, R. J.; Buda, F. *J. Am. Chem. Soc.* **1998**, *120*, 7174.

(7) Hansen, S. M.; Rominger, F.; Metz, M.; Hofmann, P. *Chem. Eur. J.* **1999**, *5*, 557.

(8) Adlhart, C.; Hinderling, C.; Baumann, H.; Chen, P. *J. Am. Chem. Soc.* **2000**, *122*, 8204.

(9) Sanford, S. S.; Love, J. A.; Grubbs, R. H. *J. Am. Chem. Soc.* **2001**, *123*, 6543.

(10) Cavallo, L. *J. Am. Chem. Soc.* **2002**, *124*, 8965.

(11) Frisch, M. J.; Trucks, G. W.; Schlegel, H. B.; Scuseria, G. E.; Robb, M. A.; Cheeseman, J. R.; Zakrzewski, V. G.; Montgomery, J. A., Jr.; Stratmann, R. E.; Burant, J. C.; Dapprich, S.; Millam, J. M.; Daniels, A. D.; Kudin, K. N.; Strain, M. C.; Farkas, O.; Tomasi, J.; Barone, V.; Cossi, M.; Cammi, R.; Mennucci, B.; Pomelli, C.; Adamo, C.; Clifford, S.; Ochterski, J.; Petersson, G. A.; Ayala, P. Y.; Cui, Q.; Morokuma, K.; Malick, D. K.; Rabuck, A. D.; Raghavachari, K.; Foresman, J. B.; Cioslowski, J.; Ortiz, J. V.; Stefanov, B. B.; Liu, G.; Liashenko, A.; Piskorz, P.; Komaromi, I.; Gomperts, R.; Martin, R. L.; Fox, D. J.; Keith, T.; Al-Laham, M. A.; Peng, C. Y.; Nanayakkara, A.; Gonzalez, C.; Challacombe, M.; Gill, P. M. W.; Johnson, B. G.; Chen, W.; Wong, M. W.; Andres, J. L.; Head-Gordon, M.; Replogle, E. S.; Pople, J. A. *Gaussian 98*, revision A.6; Gaussian, Inc.: Pittsburgh, PA, 1998.

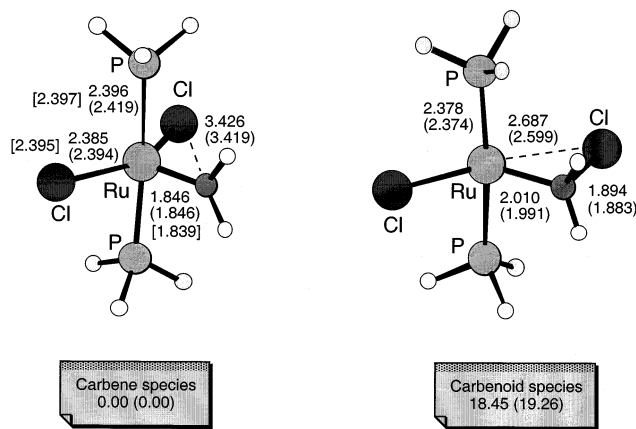


Figure 1. Schematic representation of the structure of the carbene $\text{Cl}_2(\text{PR}_3)_2\text{Ru}=\text{CH}_2$ and carbenoid $\text{Cl}_2(\text{PR}_3)_2\text{Ru}-\text{CH}_2$ ($\text{R} = \text{H}, \text{Ph}$) species (bond lengths are in angstroms and angles in degrees).

nonlocal hybrid Becke's three-parameter exchange functional¹² denoted as B3LYP. The geometry of the various critical points on the reaction surface has been fully optimized with the gradient method available in Gaussian 98 using the DZVP basis set,¹³ which is a local spin density (LSD)-optimized basis set of double- ζ quality in the valence shell plus polarization functions. A computation of the harmonic vibrational frequencies has been carried out to determine the nature of each critical point. To obtain more accurate energy values, single-point computations have been performed on the DZVP optimized structures using the 6-311G* basis set¹¹ on all atoms except ruthenium. The metal has been described by the energy-adjusted pseudopotential basis set proposed by Preuss and co-workers¹⁴ (denoted as sdd pseudopotentials in the Gaussian 98 formalism). The zero-point energy (ZPE) values obtained from the frequency computations at the DZVP level have been included in the energy computations at the 6-311G* level. For the larger system including the triphenylphosphine ligands PPh_3 , the 3-21G* basis¹¹ has been employed for all atoms.

Results and Discussion

I. Structure of the Active Species: Metal Carbene or Carbenoid Species? To elucidate the real nature of the active species, we have investigated the existence of either a metal carbene or a carbenoid species for the model ruthenium complex. We have found that both carbene and carbenoid structures are a minimum of the surface and that the former is significantly more stable ($18.45 \text{ kcal mol}^{-1}$) than the latter. The two complexes are schematically represented in Figure 1 with the values of the most relevant geometrical parameters. In the carbene complex the metal has square pyramidal coordination with the two chlorine atoms and the two PH_3 ligands approximately in the same plane and the CH_2 methylene in the apical position.

We have re-computed the structure of both complexes after replacement of the two small PH_3 fragments with two triphenylphosphine (PPh_3) ligands (new geometrical parameters in parentheses). A comparison of the two

sets of parameters shows that the increase of the steric hindrance has a negligible effect on the molecular geometry. Also, the energy difference between the two species does not change significantly, being now $19.26 \text{ kcal mol}^{-1}$. Thus these results indicate the carbenoid form as the most likely active species of the process. It is worth emphasizing that the structural features computed for the carbenoid form are in very good agreement with those experimentally determined by Grubbs and co-workers for the complex $\text{Cl}_2(\text{PPh}_3)_2\text{Ru}=\text{CHAr}$ by means of X-ray diffraction analysis (values in square brackets).^{5c} This finding indicates that the computational approach chosen here is suitable for describing this type of system.

II. Metathesis Reaction Paths: Monophosphinic or Biphosphinic Complexes? Carbene or Carbenoid Species? In this section we discuss the singlet potential energy surface (PES) associated with the reaction between one ethylene molecule and the $\text{Cl}_2(\text{PR}_3)_2\text{Ru}=\text{CH}_2$ ($\text{R} = \text{H}, \text{Ph}$) carbene complex. The existence of three different reaction pathways (path A, path B, path C), involving either carbene or carbenoid species with one (monophosphinic) or two (biphosphinic) PH_3 ligands, has been demonstrated. A schematic representation of the three reaction pathways is given in Figures 2 (paths A and B) and 3 (path C), while the structure of the various critical points located along them is reported in Figures 4 (path A), 5 (path B), and 6 and 7 (path C). A detailed description of the three paths is given in the following.

Path A. We discuss first the results obtained for the simple model system $\text{Cl}_2(\text{PH}_3)_2\text{Ru}=\text{CH}_2 + \text{ethylene}$. The first step of the process corresponds to the loss of a PH_3 ligand and the formation of a monophosphinic species (M_1). Since the energy of the system, after PH_3 removal, increases significantly ($\text{M}_1 + \text{isolated PH}_3$ is $18.86 \text{ kcal mol}^{-1}$ higher than the starting biphosphinic species $\text{Cl}_2(\text{PH}_3)_2\text{Ru}=\text{CH}_2$), the equilibrium is strongly moved to the left. Thus only a few $\text{Cl}_2(\text{PH}_3)\text{Ru}=\text{CH}_2$ molecules are available to catalyze the reaction. M_1 has a free coordination site and easily coordinates one ethylene molecule. This process does not require any barrier and leads to a new complex M_2 where the olefin has replaced one PH_3 ligand. M_2 is $8.73 \text{ kcal mol}^{-1}$ lower in energy than M_1 , but remains $10.13 \text{ kcal mol}^{-1}$ higher than reactants. This indicates that the metal-phosphine interaction is significantly stronger than that between metal and ethylene. The *trans* arrangement ($\text{Cl}-\text{Ru}-\text{Cl} = 180^\circ$) of the two chlorine atoms in M_2 is different from that proposed by Grubbs in ref 5f ($\text{Cl}-\text{Ru}-\text{Cl} = 90^\circ$). However our structure corresponds to the most stable arrangement of the various ligands after olefin coordination. The only way the olefin can approach and coordinate to the metal leads to a *trans* arrangement of the two chlorine atoms. The previously expelled PH_3 ligand enters again the metal coordination sphere, leading to a new intermediate (M_3), which still lies $5.11 \text{ kcal mol}^{-1}$ higher in energy than reactants. M_3 has a distorted octahedral structure where the phosphine, which is opposite to the ethylene, has a significantly stronger Ru-P bond (2.342 \AA) than the other PH_3 ligand (2.628 \AA). This indicates a stronger *trans* effect of the CH_2 moiety with respect to that of the ethylene molecule. The reaction path leads from M_3 to a ruthenacy-

(12) Becke, A. D. *J. Chem. Phys.* **1993**, *98*, 5648.

(13) Godbout, N.; Salahub, D. R.; Andzelm, J.; Wimmer, E. *Can. J. Chem.* **1992**, *70*, 560. *UniChem DGauss*, Version 2.3.1; Cray Research, Inc., 1994.

(14) Andrae, D.; Haeussermann, U.; Dolg, M.; Stoll, H.; Preuss, H. *Theor. Chim. Acta* **1990**, *77*, 123.

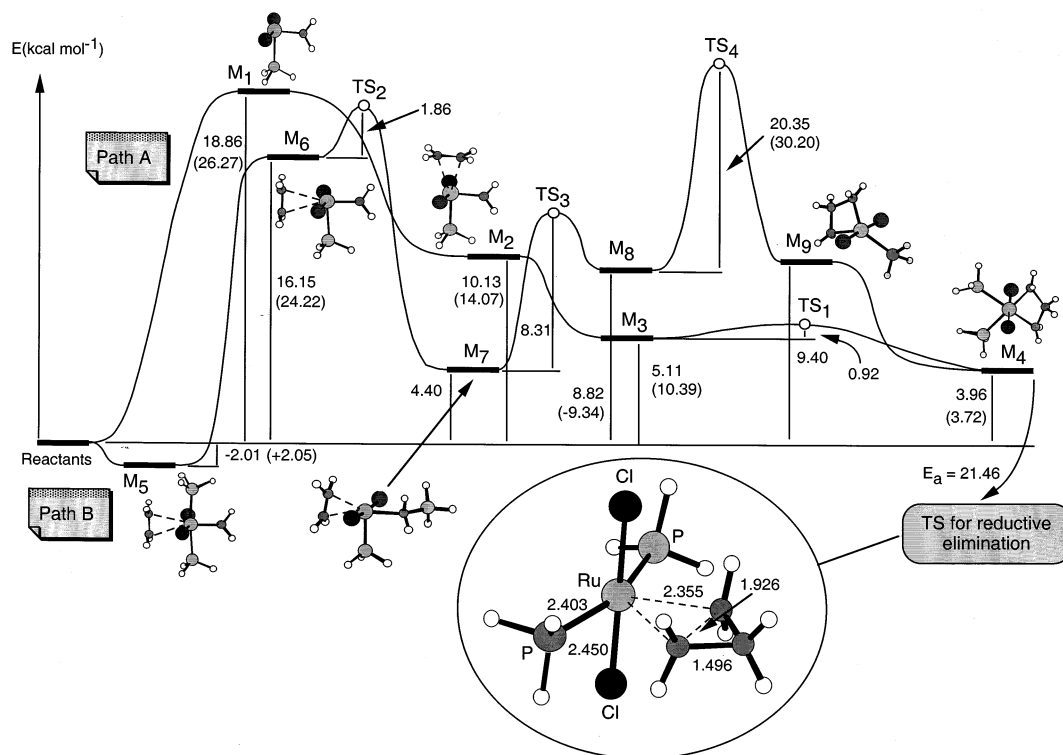


Figure 2. Energy profiles for path A and path B. In the enlargement the structure of the transition state for reductive elimination from M_4 is reported. The values in parentheses refer to the case $PR_3 = PPh_3$ (bond lengths are in angstroms and angles in degrees).

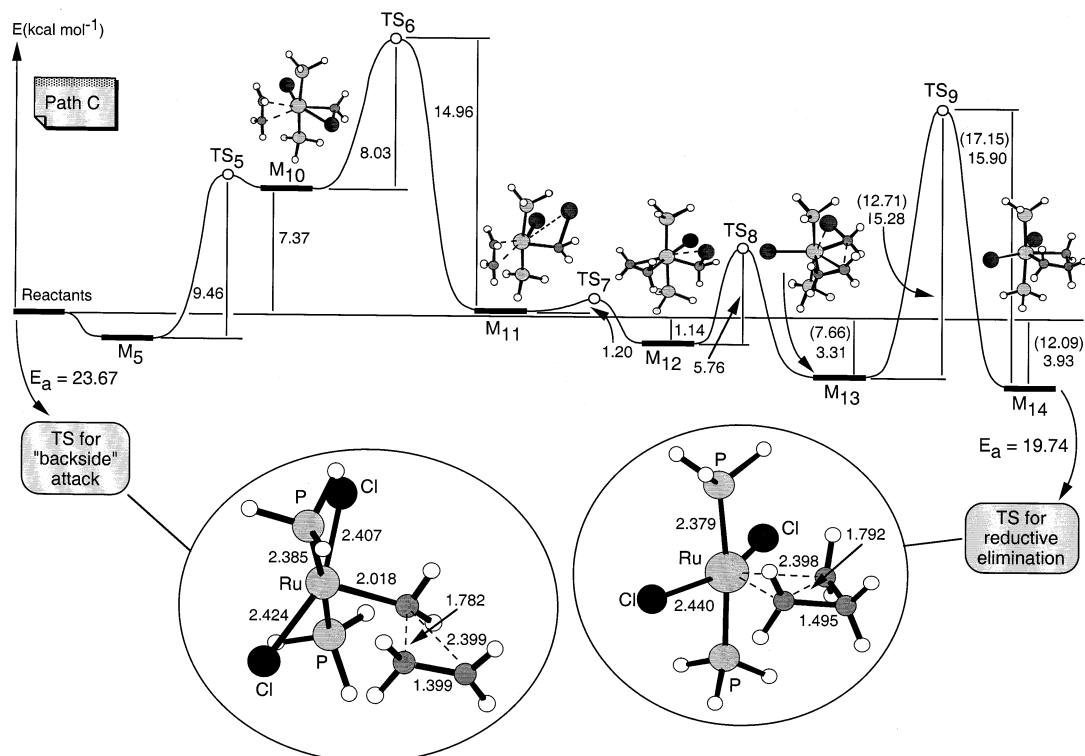


Figure 3. Energy profile for path C. In the enlargement the structures of the transition state for reductive elimination from M_{14} and for the "backside attack" are reported. The values in parentheses refer to the case $PR_3 = PPh_3$ (bond lengths are in angstroms and angles in degrees).

lobutane species (M_4) by overcoming a small energy barrier of $0.92 \text{ kcal mol}^{-1}$ (transition state TS_1). M_4 is $1.15 \text{ kcal mol}^{-1}$ more stable than M_3 and is characterized by a C_{2v} symmetry with the three carbon atoms, the metal, and the phosphorus atom lying in the same

plane. The two Ru–C bonds and the two σ C–C bonds in the cycle are now 2.022 and 1.593 \AA , respectively. The geometry of TS_1 is very similar to that of M_3 . Here the distance between the olefin carbon and the methylene carbon is still large (2.594 \AA), and only a slight

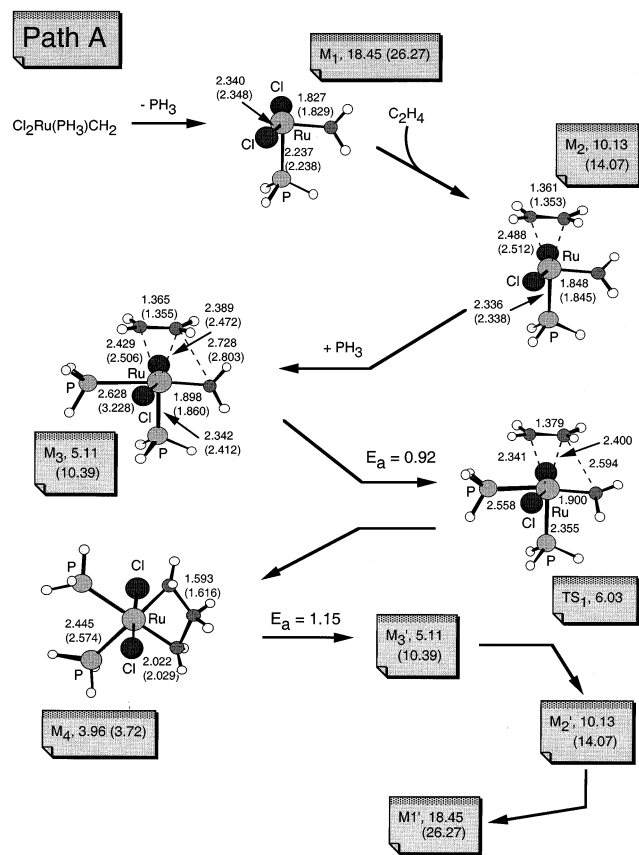


Figure 4. Schematic representation of the structures of the critical points found along path A (bond lengths are in angstroms and angles in degrees). The energy values (kcal mol^{-1}) relative to reactants ($\text{Cl}_2(\text{PR}_3)_2\text{Ru}=\text{CH}_2$ + ethylene) and the activation barriers E_a are reported. The values in parentheses refer to the case $\text{PR}_3 = \text{PPh}_3$.

lengthening of the Ru–CH₂ bond can be observed (1.898 Å in M₃ and 1.900 Å in TS₁). The transformation M₃ → TS₁ → M₄ can be formally considered a [2+2] cycloaddition involving the olefin and the Ru=CH₂ π systems. As already suggested, the interaction of the ethylene molecule with the metal orbitals removes the orbital symmetry and allows a forbidden process.

It is important to remember that, since in the model system investigated here the olefin substituents and the methylene substituents are the same (hydrogen atoms), the reactants and products of the metathesis reaction are identical (symmetric reaction). Thus, to reach the products from the ruthenacyclobutane intermediate, the previously described reaction path must be followed in the back direction. A breaking of the metallacycle M₄ (energy barrier of 2.06 kcal mol^{-1}) leads to the intermediate M₃' (=M₃) that loses the ethylene molecule, restoring the initial carbene complex M₁' (=M₁).

This reaction path has been almost completely recomputed using the more realistic model system formed by the $\text{Cl}_2(\text{PPh}_3)_2\text{Ru}=\text{CH}_2$ complex and one ethylene molecule. These additional computations confirm the existence of the M₁, M₂, M₃, and M₄ critical points and the general features of the reaction profile. The structures of these species are very similar to those determined for the simpler model system. The most relevant structural change has been observed in M₃ and M₄ and corresponds to a lengthening of the Ru–P distance, caused by the presence of the more cumbersome phenyl

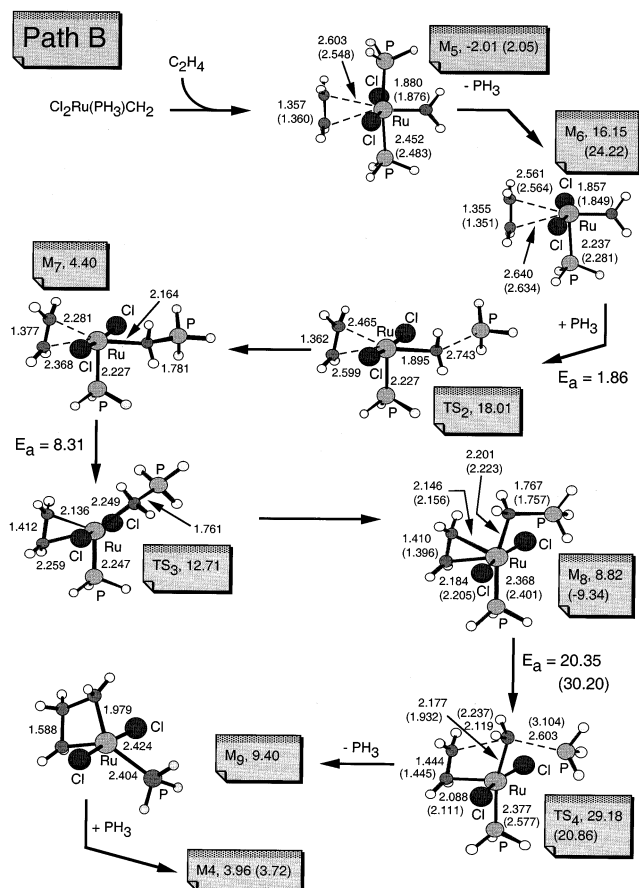


Figure 5. Schematic representation of the structures of the critical points found along path B (bond lengths are in angstroms and angles in degrees). The energy values (kcal mol^{-1}) relative to reactants ($\text{Cl}_2(\text{PR}_3)_2\text{Ru}=\text{CH}_2$ + ethylene) and the activation barriers E_a are reported. The values in parentheses refer to the case $\text{PR}_3 = \text{PPh}_3$.

groups. In M₃, for instance, the two Ru–P bonds are 2.342 and 2.628 Å in the simpler system and become 2.412 and 3.228 Å when PH_3 is replaced by PPh_3 . The energy values of the various intermediates clearly indicate a stronger Ru–P bond in the presence of the PPh_3 ligands. This is particularly evident when we consider the energy gap associated with the breaking of the Ru–P bond occurring in the first step (ejection of one phosphine ligand and formation of M₁): this value increases from 18.86 (PH_3) to 26.27 kcal mol^{-1} (PPh_3). This finding suggests that the electronic effect of replacing PH_3 with PPh_3 is dominant with respect to the steric effect.

Path B. This reaction channel involves both carbenic and carbenoid species. In the first step the ethylene molecule enters immediately the metal coordination sphere before the expulsion of one phosphine ligand. An octahedral 18-electron complex M₅, similar to M₃, is formed. In M₅ a significant *trans* effect of the CH₂ fragment on the ethylene ligand can be observed. This effect weakens the ethylene–metal bonds that become significantly longer (2.603 Å) than in M₃ (2.429 Å). It is interesting to point out that M₅ is considerably more stable than M₃ (along path A), the energy gap between the two intermediates being 7.12 kcal mol^{-1} . This is probably due to the presence in M₅ of a *trans* effect that decreases the strength of the metal–ethylene bond and

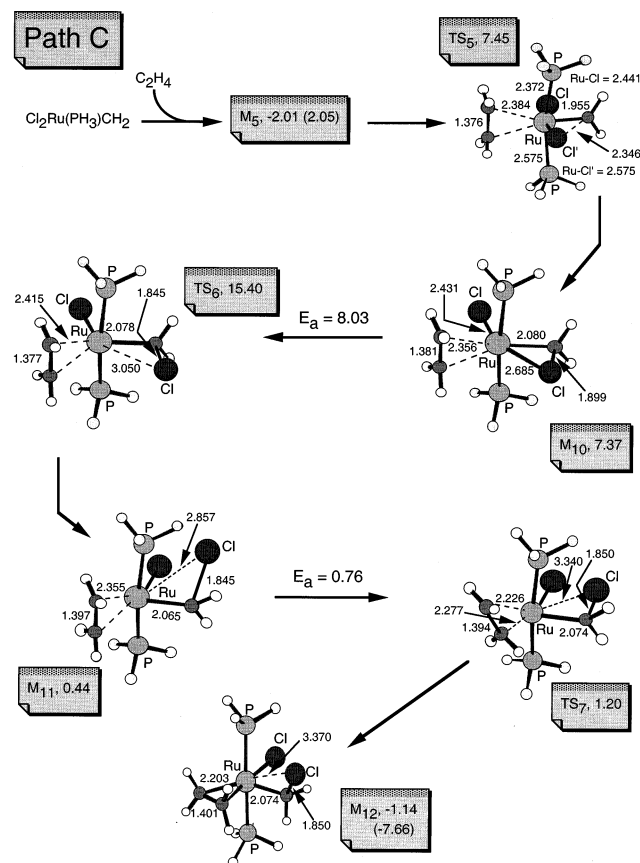


Figure 6. Schematic representation of the structures of the critical points TS₅, M₁₀, TS₆, M₁₁, TS₇, and M₁₂ found along path C (bond lengths are in angstroms and angles in degrees). The energy values (kcal mol⁻¹) relative to reactants (Cl₂(PR₃)₂Ru=CH₂ + ethylene) and the activation barriers E_a are reported. The values in parentheses refer to the case PR₃ = PPh₃.

not that of the more energetic Ru–P bond (one of the two Ru–P bonds varies from 2.628 Å in M₃ to 2.452 Å in M₅). In the second step one phosphine ligand is expelled from the metal coordination sphere to form the complex M₆, which has the same stoichiometry as M₂, but is 6.02 kcal mol⁻¹ higher in energy. A comparison of the two structures M₂ and M₆ shows that, while no *trans* effects of the methylene are possible in the former case, a *trans* effect of methylene on ethylene is found in the latter (the Ru–C distances are 2.561 Å in M₆ and 2.488 Å in M₂). This explains the computed energy gap between the two intermediates, which can be considered an estimate of the difference between the phosphine and methylene *trans* effect. Also, it is worth pointing out that the loss of one PH₃ group determines an increase of the energy of 18.16 kcal mol⁻¹, in agreement with the value found for the same transformation (Cl₂(PH₃)₂Ru=CH₂ → M₁ + PH₃) along path A. The expelled PH₃ molecule forms a new bond with the methylene moiety to afford a carbenoid intermediate M₇. This requires a small activation barrier of 1.86 kcal mol⁻¹ associated with transition state TS₂. In TS₂ the new forming C–P bond is 2.743 Å, while the Ru–C bond, which is losing its double-bond character, is 1.895 Å. This bond becomes 2.164 Å in M₇. The breaking of the π Ru–C bond and the formation of the new σ C–P bond is responsible for a significant energy stabilization: M₇ is 11.75 kcal mol⁻¹

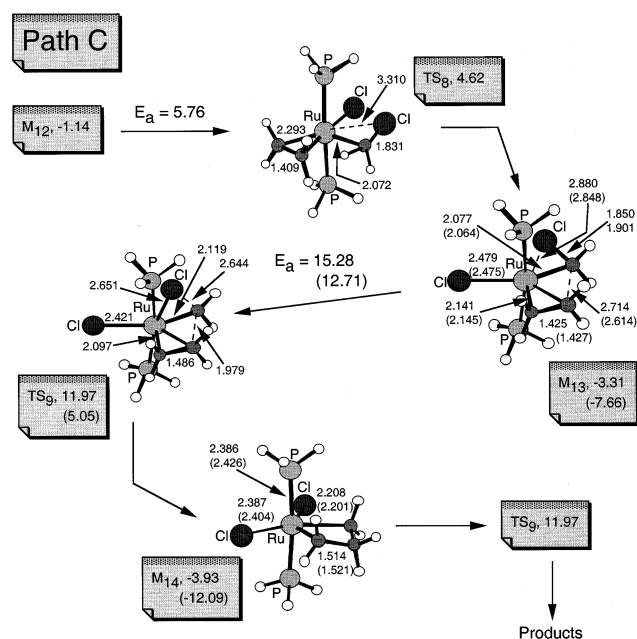


Figure 7. Schematic representation of the structures of the critical points TS₈, M₁₃, TS₉, and M₁₄ found along path C (bond lengths are in angstroms and angles in degrees). The energy values (kcal mol⁻¹) relative to reactants (Cl₂(PR₃)₂Ru=CH₂ + ethylene) and the activation barriers E_a are reported. The values in parentheses refer to the case PR₃ = PPh₃.

lower than M₆. It is interesting to note that in M₇ the loss of the Ru–C double-bond character determines a decreasing of the CH₂ *trans* effect, as is evident from the values of the two ethylene–Ru distances. These bond lengths become 2.281 and 2.368 Å. A further transition state, TS₃ (activation barrier of 8.31 kcal mol⁻¹), leads to a new carbenoid species (M₈), where the CH₂–PH₃ fragment has migrated to a *trans* position with respect to the PH₃ ligand. As a consequence of this displacement, the *trans* effect of CH₂ further decreases on the Ru–ethylene bonds, but increases on the more energetic Ru–P bond. More important, in M₈ the CH₂ unit is much closer to the ethylene ligand and from this position can move more easily toward the olefin, leading to a monophosphinic ruthenacyclobutane intermediate M₉. This species has C_{2v} symmetry, with the two chlorine atoms orthogonal to the C–C–C–Ru plane. This process requires the overcoming of a significant activation barrier (20.35 kcal mol⁻¹), mainly determined by the breaking of the C–P bond. Since M₉ has an unsaturated coordination sphere, the metal can easily accept the previously expelled PH₃ ligand and afford the biphosphinic ruthenacyclobutane M₄. Thus, the two reaction paths A and B converge to the same intermediate M₄, which can lead to the final metathesis products by following in the backward direction either path B or path A.

The structure and energy of M₅, M₆, M₈, and TS₄ have been re-computed for the species Cl₂(PPh₃)₂Ru=CH₂. As observed for path A, the structural variations are modest with respect to the simpler model system. Once again the most significant change due to the replacement of the hydrogen atoms with phenyl rings is a lengthening of the Ru–P bonds. More important are the energy variations. M₅ is now 2.05 kcal mol⁻¹ higher than

reactants, and the difference between M_5 and M_6 becomes 22.17 kcal mol⁻¹. The most relevant energy variation is observed for M_8 , which becomes 9.34 kcal mol⁻¹ lower than reactants. A reasonable explanation for the large stabilization of M_8 can be found in the interaction between the π orbitals of the phenyl groups and the unsaturated metal. In this way the free coordination site of the metal, which has five ligands, is partly saturated by the interaction with the phosphine substituents. This interaction is probably less effective in TS_4 , where one PPh_3 ligand is moving away from the CH_2 group. As a consequence, the barrier for the step $M_8 \rightarrow TS_4 \rightarrow M_9$ increases significantly (from 20.35 to 30.20 kcal mol⁻¹).

Path C. After the coordination of one ethylene molecule, the intermediate M_5 can follow a different reaction channel and can transform to a new carbenoid species (M_{10}), where one chlorine atom and not a phosphine group moves to the methylene fragment. It is interesting to note that this process does not require the expulsion of the chlorine from the metal sphere and its subsequent binding to the methylene carbon, as found for the phosphine ligand in the transformation $M_6 \rightarrow M_7$. In the present case a Cl atom undergoes a real migration from the metal to the methylene carbon (transition state TS_5) by overcoming a barrier of 9.46 kcal mol⁻¹. The different behavior observed for Cl, when compared to PH_3 , is probably due to the presence, in the former case, of two lone pairs, which allow a partial simultaneous bonding with the metal and the carbon atom. Since in M_{10} the methylene and the ethylene are on opposite sides with respect to the ruthenium, the system undergoes a structural rearrangement to place the methylene carbon closer to one olefin carbon. This transformation involves two transition states, TS_6 and TS_7 , characterized by a barrier of 8.03 and 0.76 kcal mol⁻¹, respectively, and leads to the intermediate M_{12} . Here the three carbon atoms and the metal lie in the same plane, and the distance between the methylene carbon and one olefin carbon is 2.780 Å. A further rotation around the Ru–C bond, which requires 5.76 kcal mol⁻¹, again places the chlorine atom in the C–C–C–Ru plane (intermediate M_{13}) and determines a decrease of the carbon(methylene)–carbon(olefin) distance (2.714 Å). Thus the transformation $M_5 \rightarrow M_{13}$ leads from a biphosphinic carbenic species to a slightly more stable biphosphinic carbenoid species (the M_5 – M_{13} energy gap is 1.30 kcal mol⁻¹). This energy trend is opposite that observed for the carbenic and carbenoid catalytic species reported in Figure 1, where the former is 18.45 kcal mol⁻¹ more stable than the latter. An explanation for this reversed energy trend can be found in the presence of the additional ethylene ligand. The interactions between the olefin carbons and the metal are weak in M_5 , which is characterized by a strong methylene *trans* effect, but become much stronger in M_{13} , where this *trans* effect disappears (the carbon(olefin)–metal distance becomes 2.141 Å). Also, the vacant coordination site in M_{13} and the consequent less crowded arrangement of the various ligands decrease the steric hindrance.

The next step is the formation of the ruthenacyclobutane M_{14} (C_{2v} symmetry). In this species, which is an isomer of M_4 , the two PH_3 ligands are orthogonal to the

Ru–C–C–C plane. This step requires the overcoming of an activation barrier of 15.28 kcal mol⁻¹ (transition state TS_9). A ring opening of M_{14} , occurring between the two original olefin carbons, leads, in principle, to the metathesis products. As already observed, for the simple model system considered here, where only hydrogens are bonded to the carbon atoms, the path leading from M_{14} to the products is identical to the path connecting M_5 to M_{14} . The most important barriers along this back-pathway are those associated with TS_9 (15.90 kcal mol⁻¹) and TS_6 (14.96 kcal mol⁻¹).

As observed for the two paths A and B, the computation of the two critical points M_{13} and M_{14} in the presence of the more cumbersome phenyl substituents provides very similar geometrical parameters. More interesting are the energy values of the two intermediates. The interaction of the phenyl groups with the metal, as found along path B, determines a significant stabilization of the two carbenoid complexes M_{13} and M_{14} with respect to the starting carbene species M_5 . A large stabilization is found for the point TS_9 also. The final effect is a lowering of the activation energy for the transformation $M_{13} \rightarrow TS_9 \rightarrow M_{14}$ that becomes 12.71 kcal mol⁻¹. The barrier for the reverse transformation $M_{14} \rightarrow TS_9 \rightarrow M_{13}$ changes to 17.15 kcal mol⁻¹.

These results and those previously discussed for path B indicate two main factors, which can make the carbenoid species more stable than the corresponding carbene complexes (compare M_{13} and M_{14} to M_5 along path C and M_8 to M_5 along path B). These are (1) a stronger metal–olefin interaction which becomes possible when the *trans* effect of the CH_2 fragment decreases; (2) a free coordination site on the metal that can be partially saturated by the phosphine substituents (the phenyl groups in the present case). It is interesting to note that the relevant stabilization obtained for the carbenoid species could explain the experimentally observed increasing reaction rate when cumbersome and electron-donor phosphine groups are used.

A comparison between the three reaction pathways points to path A and path C as the most likely channels leading to the metathesis products since it requires the overcoming of modest energy barriers. It is interesting to outline that path C does not predict the formation of active monophosphinic carbenic species as suggested by Grubbs to explain the decreasing reaction rate when high concentrations of phosphines are used. However, an alternative explanation, which is compatible with the features of path C, can be proposed. Path C is characterized by four migration processes of the chlorine atom: $M_5 \rightarrow M_{10}$ and $M_{13} \rightarrow M_{14}$ in the forward direction and $M_{10} \rightarrow M_5$ and $M_{14} \rightarrow M_{13}$ in the backward direction. It is conceivable to believe that an excess amount of the phosphine species in the reaction mixture can compete with the migrating chlorine atoms and determine a lowering of the reaction rate.

III. Competition between Metathesis and Cyclopropanation. To investigate the competition between metathesis and cyclopropanation, we have examined either the direct attack of the olefin on the methylene unit of the carbenic species $Cl_2(PH_3)_2Ru=CH_2$ (“backside” attack) or the reductive elimination process starting from the two isomeric metallacycles M_4 and M_{14} . The transition state for the “backside” attack is schemati-

cally represented in Figure 3. This structure is characterized by a strong interaction between the methylene carbon and one olefin carbon (1.782 Å), which is responsible of a significant lengthening of the Ru–C bond (2.018 Å). Since the corresponding activation barrier (23.67 kcal mol⁻¹) is higher than those associated with the metathesis pathways, this channel is ruled out from the mechanistic possibilities.

The two transition states for the reductive elimination are shown in Figure 2 (for M₄) and Figure 3 (for M₁₄). Both transition states have a strong product-like character with the cyclopropane ring almost completed. The corresponding activation energies are again larger (21.46 and 19.74 kcal mol⁻¹, respectively) than those required by the metathesis. Thus these two channels also are quite unlike on energy grounds.

Conclusion

In this paper we have carried out a theoretical investigation at the DFT (B3LYP) level of the mechanism of the metathesis reaction catalyzed by Grubbs' complexes. The model system is formed by one ethylene molecule and the Cl₂(PH₃)₂Ru=CH₂ complex which emulates the Grubbs' catalyst. To validate this simple model, several critical points have been re-computed for the complex Cl₂(PPh₃)₂Ru=CH₂. The results that we have obtained are relevant since they have elucidated the nature of the active species and have provided an exhaustive mechanistic scenario for these processes. The most important points can be summarized as follows.

(i) The starting active catalytic species is a metal-carbene (PH₃)₂Cl₂Ru=CH₂ and not a carbenoid complex (PH₃)₂ClRu–CH₂Cl, which is significantly higher in energy (18.45 kcal mol⁻¹) than the former. We indicate these species as “primary” active catalytic species. These results have been confirmed by the computations carried out on the larger model system including phosphine ligands.

(ii) The existence of three different reaction pathways has been demonstrated. Our results indicate that paths A and C are the most likely reaction channels to obtain the metathesis product. Path A is similar to the “dissociative” path proposed by Grubbs and recently computed by Cavallo.¹⁰ However, in the present case we have shown that, after olefin coordination, the expelled phosphine ligand again coordinates the metal, leading to an 18-electron bis-phosphine ruthenacyclobutane intermediate. Path C is characterized by the presence of carbenoid complexes, where a chlorine atom has migrated from the metal to the methylene carbon. These species, after olefin coordination, become slightly more

stable than the corresponding carbenic forms. Their stability further increases when phenyl rings replace the phosphine hydrogens. This can be explained by the interaction of the π orbital system of these substituents with the metal coordination vacant site. Thus these carbenoid complexes would represent “secondary” active species, which play a key role in the formation of a metallacyclobutane intermediate. Their stability and importance should increase when cumbersome and electron-donor groups are involved in the phosphine groups.

(iii) The mechanistic scenario that stems from this computational evidence is somewhat different from that proposed by Grubbs, who suggested a monophosphinic carbenic complex (PH₃)Cl₂Ru=CH₂ as real active species for the metathesis. We have found that these species are involved only in one reaction pathway (path A), while bis-phosphine carbenic complexes represent the active species for the other reaction channel (path C). This finding could explain the results obtained by Hofmann,⁷ who proposed, for his catalysts, bis-phosphine complexes as active species.

(iv) The nature of the ruthenacyclobutane has been elucidated. This species is not a transition state, but a real intermediate on the reaction surface, which becomes particularly stable in the presence of tri-phenylphosphine ligands.

(v) We have demonstrated the existence of three paths leading to the cyclopropane product. One is a direct attack of the olefin on the methylene carbon, and the others correspond to reductive elimination processes. In all three cases the cyclopropanation is disfavored since it requires the overcoming of larger activation barriers than those found for the metathesis.

Acknowledgment. We would like to thank CNR and MURST (Progetto Nazionale “Stereoselezione in Sintesi Organica: Metodologie ed Applicazioni”) and Bologna University (funds for selected research topics) for the financial support of this research.

Supporting Information Available: Table S1: Cartesian coordinates (Å), total energies (Hartree), and zero-point energies (ZPE, Hartree) obtained with the DZVP basis set and total energies (Hartree) obtained with the 6-311G*/sdd basis set for the various critical points computed for the model system Cl₂(PH₃)₂Ru=CH₂ + ethylene. Table S2: total energies (Hartree) obtained with the 3-21G* basis set for the various critical points computed for the model system Cl₂(PPh₃)₂Ru=CH₂ + ethylene. This material is available free of charge via the Internet at <http://pubs.acs.org>.

OM020536O